Journal of the Chinese Society of Mechanical Engineers, Vol.47, No.2, pp 103~112 (2026)

Design Improvement and Strength Analysis of a Pin Lock Structure for Wind Turbine Hub

Rong-Mao Lee*, Jien-Chen Chen**, Nelson T. Corbita Jr.*** and Jui-Hung Liu****

Keywords: Wind Turbine, Operation and Maintenance, Pin Lock, Load Analysis.

ABSTRACT

This study presents an analysis and design improvement of the hub pin lock structure in a 2 MW wind turbine, addressing a critical malfunction caused by prolonged exposure to extreme wind conditions over 15 years of operation. The redesign focuses on enhancing the durability and reliability of the pin support base, using 3D modeling, structural strength analysis, and fatigue analysis based on Miner's rule. The redesigned pin lock was evaluated for its ability to withstand cyclic loading conditions through load simulations under various wind scenarios. The cumulative fatigue damage was calculated, confirming that the structure remains well below the failure threshold, ensuring long-term performance. The proposed design reduces wind turbine downtime and maintenance costs, offering significant implications for improving the reliability of wind turbine components and extending their operational life.

INTRODUCTION

The cost of energy (COE) is an index to evaluate the economic performance of wind farm operations. This index comprises the initial capital cost, the regular annual charge rate, the annual energy production, and the operation and maintenance (O&M) cost.

The average percentage of O&M costs in the COE for offshore wind farms may reach up to 25–30% according to Feng et.al. (2010). Figure 1 shows the result of a survey of failure rate and downtime for two European wind farms conducted by Crabtree (2010). Over 20000 years of data on wind turbines (WT) are included in this investigation. Due to the lengthy WT downtime per failure, quantitative studies were devoted to the reliability of mechanical components, such as the gearbox or blades. The WT downtime per failure in Taiwan is much longer than that in Europe because Taiwan is far from these WT manufacturers.

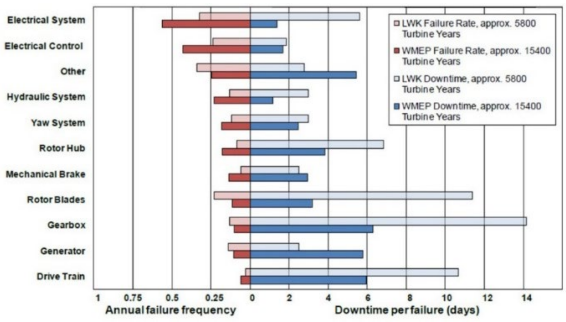

Fig. 1. WT failure rate and downtime per failure

Among the mechanical components, the mechanical brake is highly relevant to WT O&M. The wind turbine guidelines (GL) suggest the WT lock system shall be capable of holding the blades, the rotor, and the nacelle against an annual gust and a gust during maintenance. The WT lock devices include the yaw lock system and the rotor lock system, as shown in Figure 2 from Kang & Lee (2017). The yaw lock system stops the nacelle and stabilizes its position. The rotor lock system can be divided into the disc brake and the hub pin lock. The disc brake (referred to as the rotor brake and rotor disc in Figure 2 is designed for emergency stop and WT maintenance. The hub pin lock, referred to as the rotor lock in Figure 2, is a critical link in the safety chain, such as the turbine erection and WT maintenance. Once the disc brake

Paper Received December 2024. Revised May 2025. Accepted July, 2025. Author for Correspondence: Jui-Hung Liu

**Associate Professor, Department of Intelligent Automation Engineering, National Chin-Yi University of Technology, Taichung, Taiwan 411030*

***Senior Engineer, Mechanical and Mechatronics Systems Research Lab, Industrial Technology Research Institute, Hsinchu, Taiwan 310401*

****Faculty, Mechanical Engineering Department, University of Science and Technology of Southern Philippines, Cagayan de Oro City, Philippines 9000*

*****Associate Professor, Department of Intelligent Automation Engineering, National Chin-Yi University of Technology, Taichung, Taiwan 411030*

stops the WT rotor, the hub pin lock can then be activated. The function of the hub pin lock is to securely fasten the WT hub so maintenance can be carried out safely.

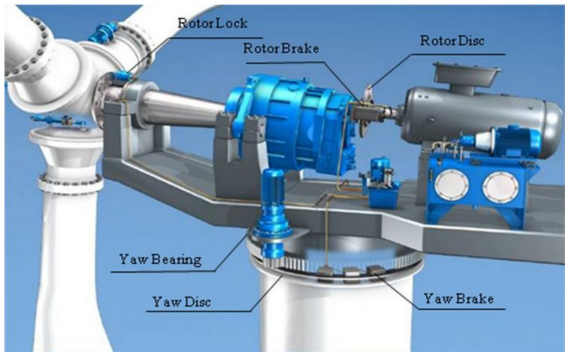

Fig. 2. Braking system of a wind turbine.

Since brake failures produce significant WT downtime and cost, an experimental study of the WT drive train was conducted by Mohamed et.al. (2019) to investigate the influence of environmental conditions on the mechanical brake behaviors. The rotor disc brake is placed next to the gearbox to reduce the speed of the generator. Since the brake force is applied to the WT rotor by a brake clamp, the mechanical properties of the brake pad and disc must be investigated under WT operation based on IEC standards (2005) and Travaglia & Lopez (2014). The structure of the WT disc brake is like that of highly developed automobiles. Therefore, the main design concerns against disc brake are the friction coefficient, the maximum braking torque, the structure strength, and the influence of temperature as stated in the studies of Talati (2009), Abhang & Bhaskar (2014), Deshpande (2015), Belhocine & Abdullah (2014) and Kang & Lee (2016).

The hub pin lock is rarely discussed compared to the yaw lock system and the rotor disc brake. The hub pin lock is a bolt linked and embedded into the lock disc mechanically, hydraulically, or electrically, as shown in Figure 3. Augusto et.al. (2016) performed the optimization design of the WT rotor lock disc. The machine load calculation was derived from GH Bladed software based on a 2.5 MW direct-drive WT. The maximum tensile stress, internal stress, maximum deformation, and safety factors were calculated in terms of the theoretical stress concentration factor. The configurations of the rotor lock disc were optimized to fulfill a safety factor of unity using an exhaustive search method and the software *COSMOS Works*.

This work focuses on analyzing and improving the hub pin lock mechanism in a 2 MW wind turbine installed on the midwestern coast of Taiwan. After over 15 years of operation, the turbine experienced a critical failure in the hub pin lock, leading to a shutdown as regular maintenance was no longer feasible. Using this real-world case as the research object, we propose a redesign to address the failure. Guided by the principles of Reliability-Centered Maintenance (RCM), this study aims to optimize the reliability of this critical component. By enhancing the design of the hub pin lock, we seek to reduce wind turbine downtime and improve operational efficiency, which are key objectives of RCM practices across industries. The redesigned structure is evaluated through load simulations and fatigue analysis to ensure long-term durability under extreme wind conditions based on Moubray (2001) and Jardine et.al. (2006).

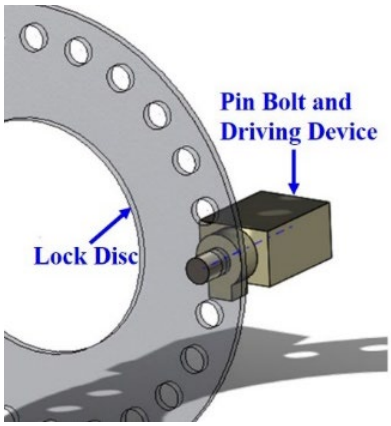

Fig. 3. Illustration of a hub pin lock.

RESEARCH OBJECT AND MOTIVATION- BREAKDOWN OF HUB PIN LOCK

In the current wind turbine (WT) model, the hub pin lock mechanism is critical to secure the rotor during maintenance. This system typically consists of pin locks on either side of the rotor - one on the left and one on the right. The exterior appearance and operational state of these pin locks are depicted in Figure 4a, providing a view of a pin lock in normal condition. Figure 4b illustrates a damaged pin lock mechanism. Further detailed imagery of the specific damage is presented in Figure 5, offering a closer examination of the compromised areas.

The photographs underscore that the pin lock mechanism has failed to withstand the load imposed by wind conditions, leading to deformation and fracture of the bolt and its pin support base. The illustration of the ruptured pin support base is depicted in Figure 6. Instead of the replacement of the entire support set of the hub pin lock, the wind farm operator demands a redesign of the pin support structure to provide adequate strength against the maximum wind speed in this wind farm. This failure has prompted a re-evaluation of the pin lock's design, with an imperative to develop a new mechanism that meets the requirements of maximum wind load resistance specific to this wind farm.

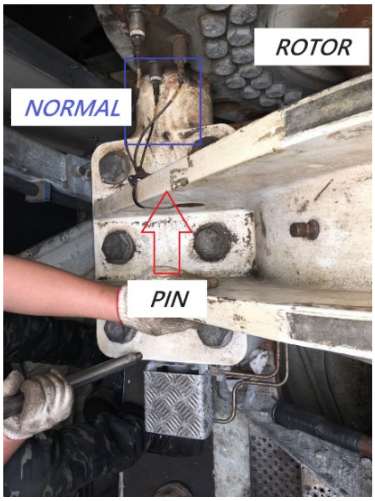

(a)

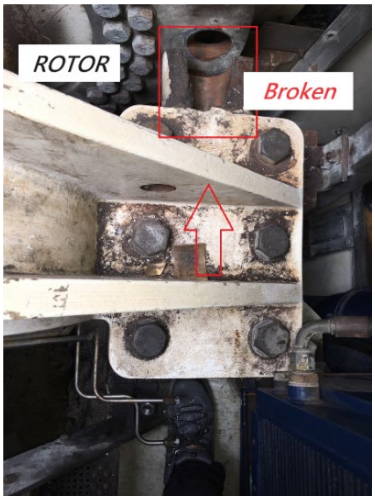

(b)

Fig. 4. (a)The lock pin mechanism at the RIGHT side (the normal one), (b) the lock pin at the LEFT side (the broken one)

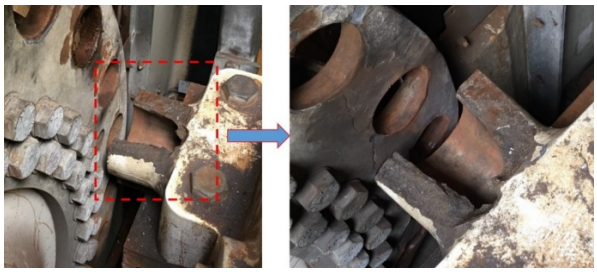

Fig. 5. Actual conditions of the broken pin support base.

Following the problem description, conducting a comprehensive force analysis to redesign the structure is crucial. This analysis will ensure that the new structure can withstand the dynamic wind conditions expected in the future. To achieve this, we will analyze the loads and stresses the pin lock mechanism is subjected to during extreme wind events, which will inform the redesign to enhance resilience and reliability.

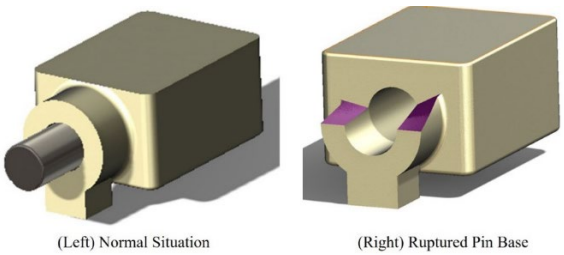

Fig. 6. Illustration of rupture pin support base.

RESEARCH METHODOLOGY

The research methodology was divided into three phases: force simulation, mechanism design, and stress analysis. Each phase was integral to developing a robust and reliable hub pin lock mechanism.

Extreme Load Simulation

The initial phase involves software simulations to determine the forces exerted on the pin lock mechanism under various wind conditions. We aim to understand the maximum stress limit that the structure can withstand. For this, we have established two separate tables to articulate our simulation parameters and design scenarios: Table 1 outlines the basic specifications of the wind turbine, providing a foundational understanding of the designated turbine.

Table 1: Basic Specification of the Wind Turbine.

Item	Value
Rated Capacity	2.0 MW
Rotor Diameter	80 m
Blade Number	3
Rated Wind Speed	13 m/s
Cut-in Wind Speed	4 m/s
Cut-out Wind Speed	25 m/s
Power Regulation	Variable Pitch
Hub Height	78 m

Table 2 details the specific wind conditions used as inputs for our simulations. These conditions are designed to estimate the maximum load the pin lock might endure. When the pin lock is engaged, we assume a parked state for the wind turbine during maintenance. The scenarios considered include wind speeds of 10 m/s, 15 m/s, and 20 m/s, with wind directions varying from 0 to 360 degrees. Additionally, we simulate various rotor azimuth angles from 0 to 180 degrees to encompass a comprehensive range of

operational states. Finally, a total of 72 simulation cases will be executed by the professional and certified software Bladed to observe the load on the rotor exerted on the hub.

Table 2: Simulation parameters for Hub Load.

Parameter	Value or Definition
Turbine Status	Parked (for maintenance)
Wind speed	10 m/s, 15 m/s, 20 m/s (**3 cases**)
Wind direction	0 to 360 with a step of 45 degrees (**8 cases**)
Rotor azimuth	0, 180, and 90 degrees (**3 cases**)
Brake torque	1200 kNm brake torque
Software	DNV-GL Bladed (version 4.2)
Simulation Duration	60 s
Total Cases Executed	Totally 72 cases (**3*8*3=72**)
Observed Outputs	Moment (M_x, M_y, M_z)
Coordinates	Refer to Figure 7

To ensure realistic simulation settings, the selected wind speeds (10 m/s, 15 m/s, 20 m/s) were cross-referenced with regional wind conditions observed at Taiwan's west coast offshore wind farms. According to wind resource assessment reports by the Taiwan Power Company (2022) and the Bureau of Energy (2023), mean annual wind speeds range from 7 to 10 m/s at hub height, while gust events during typhoon seasons can temporarily push wind speeds up to 20–25 m/s. Therefore, the selected parameters accurately represent maintenance conditions and potential extreme loading scenarios experienced by local wind turbines.

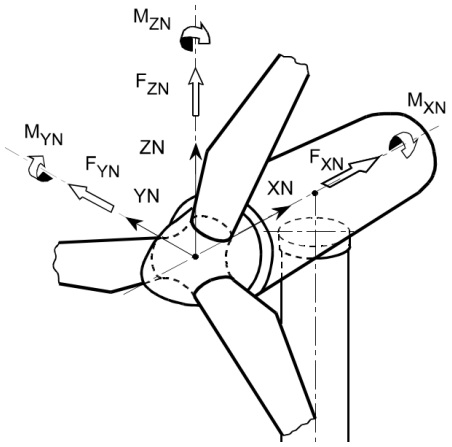

Fig. 7. Coordinate system of the wind turbine hub used for load moment analysis.

Mechanism Design

Following the simulations, we will design a new hub pin lock structure. This design phase is informed by the insights gained from the force simulation, ensuring the new mechanism can withstand the identified extreme conditions. The redesigned pin support base is demonstrated in Figure 8. The notation "CW" refers to clockwise and defines rotational direction. The dimensions of the proposed design (1st version) are illustrated in Figure 9.

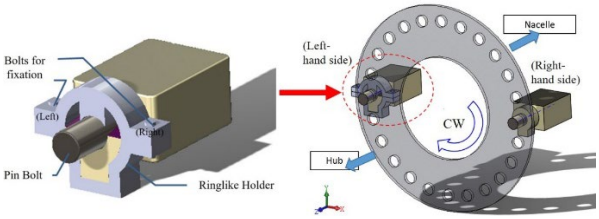

Fig.8. Redesigned pin support base.

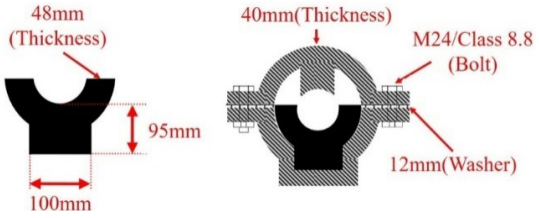

Fig.9. Dimensions of the proposed design (1st version).

Mechanism Stress Analysis

The redesigned pin lock mechanism will undergo a rigorous stress analysis using analysis software. This step is vital to validate the strength and capacity of the structure, confirming its ability to endure the loads ascertained from the simulations. The meshed models of the components for the entire WT hub pin lock structure are shown in Figure 10. The mesh details of individual components are listed in Table 3.

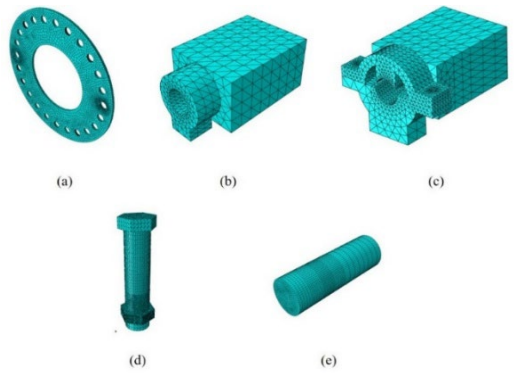

Fig. 10. Meshed model of hub pin lock: (a) lock disc; (b) pin support base; (c) redesigned pin support base; (d) bolt for fixation; (e) pin bolt.

Table 3: Mesh details of individual components.

Component	Element Type	Component*	Element Type
Left pin bolt	C3D8R	Right pin bolt	C3D8R
Top cover of ringlike holder	C3D10M	The right pin support base	C3D10M
Bottom cover of ringlike holder	C3D10M	Lock disc	C3D8R
Bolts for fixation	C3D10M	Left pin support base	C3D10M

* The direction of the left-hand side and the right-hand side is according to Figure 8.

RESULTS

The results presented in this section are based on a comprehensive series of simulations and analyses performed to evaluate the structural integrity and durability of the redesigned hub pin lock. These analyses include extreme load simulations under various wind conditions and detailed stress and fatigue evaluations. The objective is to verify that the new design can withstand the operational demands, particularly in high-load scenarios, while ensuring long-term reliability. The following subsections detail the outcomes of these simulations and analyses, explicitly focusing on the maximum load conditions, stress distributions, and cumulative fatigue damage.

Simulation Results

The WT is assumed to be in parked status (referred to Table 2) to estimate the basic response of the WT structure against loadings. The steady loads under various wind directions are shown in Figure 11. Maximal moments are observed in the Mx direction (referred to in Figure 7) when there is a misalignment between the WT hub and wind direction that is roughly 90 or 270 degrees. The influence of azimuth angles on the loadings of the hub is performed as shown in Figure 12. The maximal moment exerted on the hub is also observed in the Mx direction. The applied wind speed is 20 m/s for both.

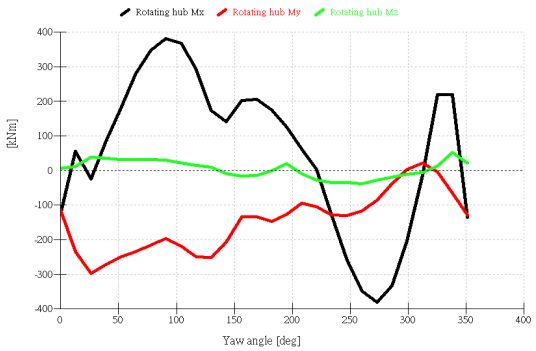

Fig. 11. Steady loads exerted on the hub under various wind directions.

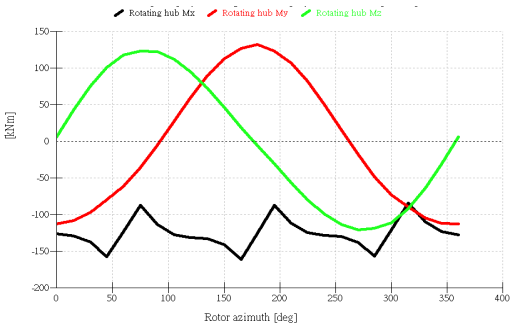

Fig. 12. Steady loads exerted on the hub under various azimuth angles.

Since the maximal moment load appeared in the Mx direction, intensive analyses for various load cases have been accomplished to investigate the peak moment load of the WT hub. The peak moment loads of 72 cases are shown in Figure 13. An extraordinary load (more than 5000 kNm) is observed. This case is named "**wind15-Direc90-Az90**", which means the wind speed is 15 m/s with the wind direction of 90 degrees, and the azimuth angle of the rotor is 90 degrees. The detailed analysis result of case "wind15-Direc90-Az90" is shown in Figure 14. Since the moment load by the wind is beyond the brake torque (referred to table 2), the rotor is still rotating (the rest threshold is below 0.05 RPM). Among all the simulation results (much more than 72 cases), extraordinary loads are mostly observed against the azimuth angle of 90 degrees.

Due to the strength limitation of brake torque (referred to in Table 2), the cases in which the corresponding peak loads are below the brake torque are included in the following discussion. As a result, a total of 48 cases from Figure 13, as shown in Figure 14, are employed for the redesign of the hub pin lock. Partial results of peak loads among these cases (Figure 14) are listed in Table 4. The worst case at WT parked position is "**wind20-Direc90-Az0**". This case is referred to as a wind coming from the east side with the azimuth angle of zero degrees. A moment load of **761.5 kNm** in M_x direction will have arisen under a 20 m/s wind speed.

WT Hub Pin Lock Mechanism

Two conditions, which are high-load conditions and normal conditions, are defined for the following analyses based on the results of Figure 14 and Table 4. The high-load condition is referred to as load case "wind20-Direc90-Az0", which is the highest load case under 20 m/s wind speed among Figure 14. The normal condition is assumed at a wind speed of 15 m/s. As a result, the highest load case "wind15-Direc0-Az0" is employed. The load parameters and the degree of freedom of individual components for simulations are listed in Tables 5 and 6, respectively.

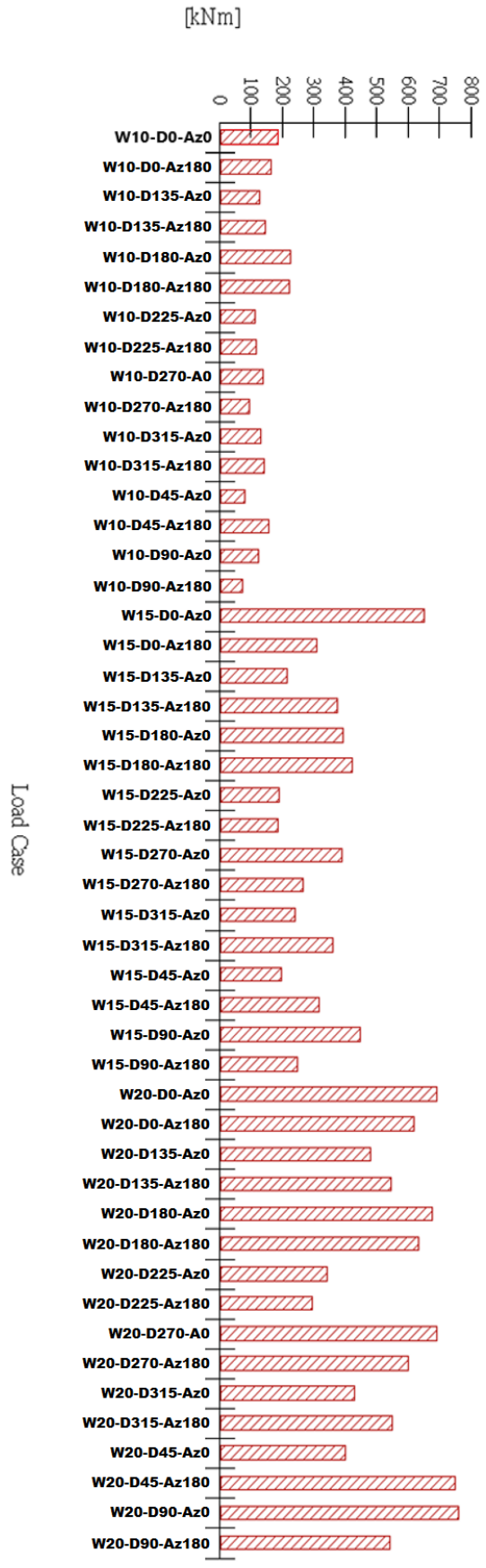

Fig. 13. Maximal moment load (in M_x direction) of various load cases.

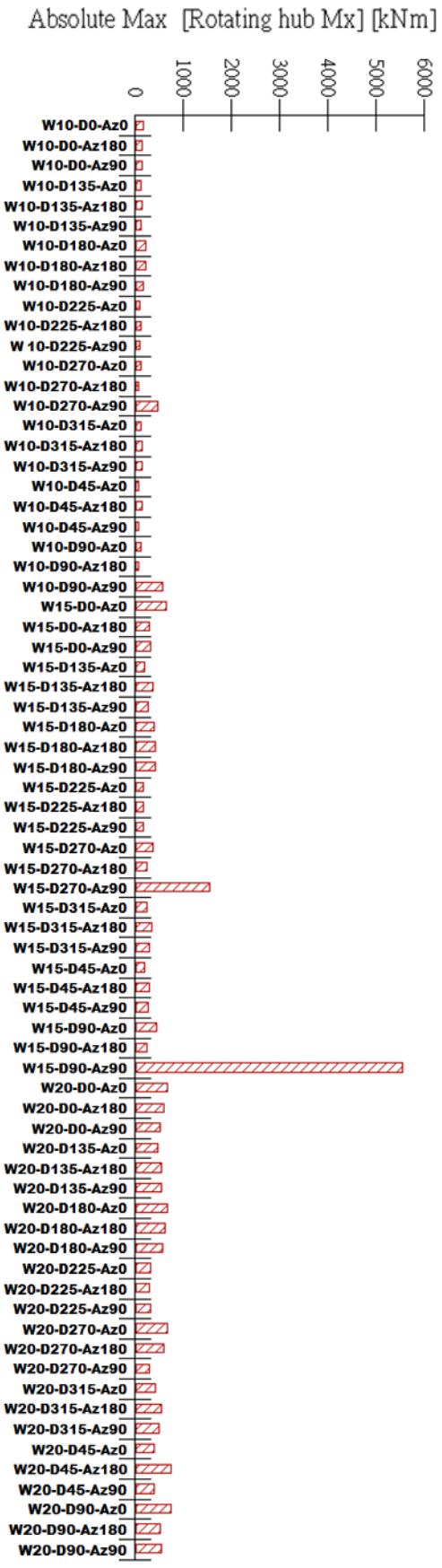

Fig. 14. Maximal moment load (in M_x direction) of 48 cases.

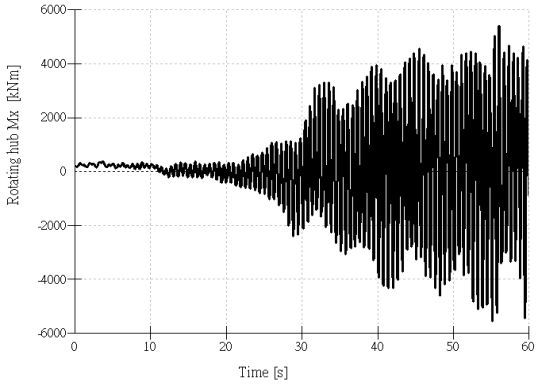

Fig. 15. Moment variation over time (Mx) for load case "wind15-Direc90-Az90"; illustrating critical loading pattern.

Table 4: Partial peak loads among cases of Figure 14.

Load Case	M_x (kNm)	M_y (kNm)
wind20-Direc90-Az0	**761.5**	-318.2
wind20-Direc0-Az0	**-691.4**	-33.7
wind20-Direc45-Az180	320.2	**433.6**
wind20-Direc90-Az0	559.7	**-597.5**

Table 5: Load parameters for structure strength simulations.

Case No.	Torque Direction*	Applied Torque (Nm)
A	CW	7.61+E8
B	CCW	7.61+E8
C	CW	6.51+E8
D	CCW	6.51+E8

* CW is referred to as clockwise, and CCW means counterclockwise. The definition of rotation direction is demonstrated in Figure 8.

Table 6: Degrees of freedom of individual components.

Component	X	Y	Z	XX	YY	ZZ
Right pin bolt	Free	Free	0	Free	0	Free
Right pin support base	0 *	0	0	0	0	Free
Lock disc	0	0	0	0	0	Free
Left pin bolt	Free	Free	0	Free	0	Free
Left pin support base	0	0	0	0	0	Free
Ringlike holder	Free	Free	Free	Free	Free	Free
Bolts for fixation	Free	Free	Free	Free	Free	Free

* ”0” means “fixed”.

Analysis Results of Structure Strength

The maximum stress inside individual components and the corresponding safety factors under CW and CCW rotation are listed in Tables 7 and 8, respectively. For the current design, the specification of fixation bolts (M24/Class 8.8) is not qualified under CW rotation. Partial simulation results are shown in Figure 16.

Table 7: Maximum stress inside components under CW rotation.

Component	Max Stress (MPa)	Safety Factor
Right pin bolt	334	2.32
Right pin support base	475	1.63
Lock disc	405	1.91
Left pin bolt	275	2.82
Left pin support base	381	2.03
Ringlike holder	430	1.80
Bolt for fixation (left)	**891**	**0.74**
Bolt for fixation (right)	**883**	**0.75**

Table 8: Maximum stress inside components under CCW rotation.

Component	Max Stress (MPa)	Safety Factor
Right pin bolt	248	3.13
Right pin support base	488	1.59
Lock disc	402	1.93
Left pin bolt	251	3.09
Left pin support base	31	25.00
Ringlike holder	468	1.66
Bolt for fixation (left)	31	25.00
Bolt for fixation (right)	18	43.06

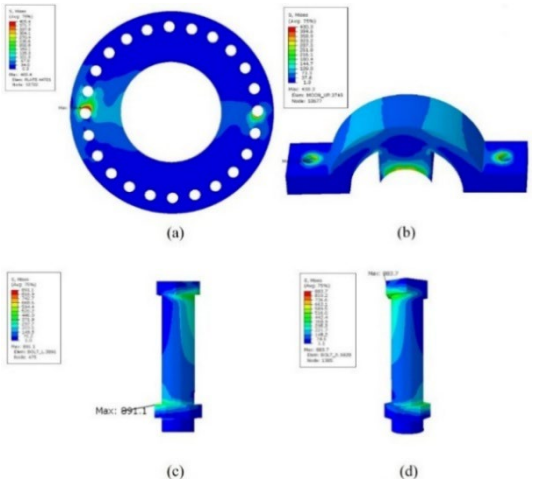

Fig. 16. Partial simulation results under CW rotation: (a) lock disc; (b) top cover of the ringlike holder; (c) left bolt for fixation; (d) right bolt for fixation.

Improvement of Proposed Design

The specification of the fixation bolt for the ring-like holder is M24 with a grade of class 8.8. According to the analysis results presented in Tables 7 and 8, the equipped fixation bolts are not sufficient for the design requirement. For the replacement of fixation bolts, analyses for two types of bolts have been accomplished, as shown in Tables 9 and 19.

Table 9: Safety factor of fixation bolt against wind speed of 20 m/s.

*Rotational direction: CW *Wind speed: 20 m/s			Safety Factor Class		
Size	**Component***	**Max Stress(MPa)**	**8.8**	**10.9**	**12.9**
M24	Right	883	**0.75**	1.06	1.25
	Left	891	**0.74**	1.05	1.23
M30	Right	281	2.35	3.35	3.91
	Left	382	1.73	2.46	2.88

* The definition of component is indicated in Fig. 9.

Table 10: Safety factor of fixation bolt against wind speed of 15 m/s.

*Rotational direction: CW *Wind speed: 15 m/s			Safety Factor Class		
Size	**Component***	**Max Stress(MPa)**	**8.8**	**10.9**	**12.9**
M24	Right	755	**0.87**	1.25	1.46
	Left	763	**0.87**	1.23	1.44
M30	Right	240	2.75	3.92	4.58
	Left	327	2.02	2.87	3.36

* The definition of component is indicated in Fig. 9.

The safety factors of M30 bolts are much higher than those of M24 bolts. Since M30 is the largest size for the bolt due to the proposed structure design, the M24 bolts have been replaced by M30 bolts in the modified design. The prototype of the modified design is shown in Figure 17. Figure 18 is the implementation of the new design for the operating turbine, which is finally complete.

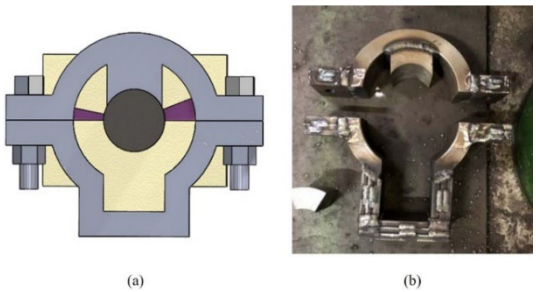

Fig. 17. Modified design: (a) structure diagram; (b) prototype.

Given the repeated cyclic loading conditions to which the pin lock is subjected, fatigue analysis plays a critical role in determining the long-term durability of the structure. Fatigue theory, particularly Miner's rule (1945), can be applied to predict the lifespan of the redesigned structure under varying wind loads, as supported by Schijve (2009).

Fig. 18. Final implementation of redesigned hub pin lock mechanism on the operational wind turbine.

Fatigue Analysis of the Pin Lock Mechanism

Given the cyclic nature of wind loading on the wind turbine hub pin lock, fatigue analysis is essential to predict the long-term durability of the redesigned structure. Fatigue damage accumulates over time, and even though each load cycle may not cause immediate failure, repeated cycles can weaken the structure and lead to eventual failure. To quantify this effect, we apply Miner's Rule, a commonly used method for cumulative fatigue damage assessment. Miner's Rule assumes that the damage caused by each stress cycle is linearly accumulated, and the structure will fail when the cumulative damage reaches a threshold value of 1. The cumulative damage D can be expressed as:

$$D = \sum_{i=1}^{n} \frac{n_i}{N_i}$$

Where:

- n_i is the number of cycles experienced at a specific stress level i,
- N_i is the number of cycles to failure at that stress level.

In this analysis, we adopt a conservative approach by assuming a 0.1 Hz frequency for significant load cycles, meaning the pin lock experiences one meaningful load cycle every 10 seconds (or 360 cycles per hour). With six maintenance events per year, each lasting 4 hours, the total engagement time for the pin lock is 24 hours, resulting in 8,640 load cycles per year. The load cycles are distributed across four wind speed ranges based on typical wind conditions during maintenance periods. The corresponding stress levels (σ) and number of cycles to failure (Ni) for each wind speed range were derived from material properties and simulation data. These are summarized in Table 11 below.

Table 11: Fatigue Estimates of the mechanism

Wind Speed	Number of Load Cycles (n_i)	Stress Level (σ) (MPa)	Cycles to Failure (N_i)	Fatigue Damage (D_i)
< 10 m/s (Low)	3,456	100	1,000,000	0.00346
10–15 m/s (Moderate)	2,592	200	125,000	0.02074
15–20 m/s (High)	1,728	300	37,000	0.04669
> 20 m/s (Very High)	864	400	15,600	0.05538

Using the S-N curve for the pin lock material and applying Miner's Rule, the cumulative damage contributions from each wind speed range were calculated, as shown in Table 1. The total fatigue damage after one year of operation was found to be:

$$D=0.00346+0.02074+0.04669+0.05538=0.12627$$

The total cumulative damage of 0.12627 is significantly below the critical failure threshold of D=1. This result indicates that the pin lock is unlikely to fail due to fatigue within one year under the current wind loading conditions. The conservative assumption of a 0.1 Hz frequency ensures that only significant load cycles are considered, capturing the most impactful variations in wind conditions during maintenance periods. The redesigned pin lock is thus expected to operate reliably over its projected service life without succumbing to fatigue-related failure.

Validation and Literature Comparison

Although experimental validation could not be performed due to practical restrictions at the operational wind farm, we cross-validated our simulation results with previous studies. Augusto et al. [12] conducted finite element analysis and load studies on a 2.5 MW wind turbine rotor lock, finding hub moments under emergency conditions reaching up to 800–900 kNm. Similarly, studies reported by Travaglia and Lopez (2014) showed mechanical brake systems subjected to comparable load magnitudes under gust conditions.

In our simulations, peak hub moments under 20 m/s wind speeds reached 761.5 kNm, aligning with published results. Furthermore, our cumulative fatigue analysis demonstrated cumulative damage far below the failure threshold, consistent with reported findings for structural components with safety factors greater than 1.5 under cyclic loading. These comparisons confirm the validity of our simulation-based approach.

CONCLUSIONS

This study provides a comprehensive analysis and redesign of a hub pin lock mechanism for a 2 MW wind turbine, addressing a critical failure observed after prolonged operation under extreme wind conditions. Through detailed load simulations, structural analysis, and applying fatigue theory using Miner's rule, the redesigned pin lock has significantly improved its durability and reliability. The fatigue analysis results demonstrate that the structure can withstand cyclic wind loads over its operational life without accumulating damaging levels of fatigue.

The cumulative damage calculations confirm that the redesigned pin lock remains within safe operational limits under typical wind conditions, ensuring its long-term functionality. These findings contribute to minimizing wind turbine downtime and maintenance costs and highlight the importance of incorporating fatigue analysis in the design phase to predict and prevent premature component failure.

By integrating fatigue theory with structural simulations, this work offers a practical framework for improving the reliability of critical wind turbine components. Future work should focus on monitoring the long-term performance of the redesigned structure in real-world conditions and exploring further optimization opportunities to enhance wind turbine maintenance strategies.

ACKNOWLEDGMENTS

The authors would like to express their appreciation to the Bureau of Energy, Ministry of Economic Affairs, the Taipower Co., and the professional wind turbine maintenance team from ITRI (Taiwan).

DECLARATION OF COMPETING INTEREST

The authors declare that they have no known competing financial interests or personal relationships that could have appeared to influence the work reported in this paper.

REFERENCES

Abhang, S.R., Bhaskar, D.P., 2014. "Design and analysis of disc brake". International Journal of Engineering Trends and Technology 8(4), 165-167.

Augusto, G.L., Culaba, A.B., Lim, L.A.G., Maglaya, A.B., 2016. "Design optimization of rotor lock disc for horizontal axis wind turbine generator". Applied Mechanics and Materials 842, 191-199.

Belhocine, A., Abdullah, O.I., 2014. "Finite element analysis of automotive disc brake and pad in frictional model contact". International Journal of Advanced Design and Manufacturing Technology 7(4), 27-42.

Bureau of Energy, Ministry of Economic Affairs, Taiwan, "Wind Resource Atlas of Taiwan", 2022 Edition.

Carroll, J., McDonald, A., and McMillan, D., "Failure rate, repair time and unscheduled O&M cost

analysis of offshore wind turbines", Wind Energy, 19(6), 1107-1119, 2016.

Crabtree, C.J., 2010. “Survey of commercially available condition monitoring systems for wind turbines”. Durham University School of Engineering and Computing Sciences and the SUPERGEN Wind Energy Technologies Consortium, Durham, UK. Technical Report.

Deshpande, A., 2015. “Development of hydraulic brake design system application”. International Journal of Research in Science and Technology 5, 61-70.

Det Norske Veritas (DNV), 2021. DNV bladed user manual, ver. 4.11. Oslo, Norway.

Feng, Y., Tavner, P.J., Long, H., 2010. “Early experiences with UK round 1 offshore wind farms”. Proceedings of the ICE-Energy 163, 167-181.

International Electrotechnical Commission, 2005. Wind turbines-part 1: Design requirements. International Standard IEC 61400-1, 3rd ed. Geneva, Switzerland.

Jardine, A.K.S., Lin, D., & Banjevic, D. (2006). “A review on machinery diagnostics and prognostics implementing condition-based maintenance”. Mechanical Systems and Signal Processing.

Kang, J.H., Lee, H.W., 2016. “The development of wind turbine brake by finite element method”. International Journal of Applied Engineering Research 11, 10294-10298.

Kang, J.H., Lee, H.W., 2017. “The development of rotor brakes for wind turbines”. International Journal of Applied Engineering Research 12, 5091-5100.

Miner, M. A. (1945). “Cumulative damage in fatigue”. Journal of Applied Mechanics.

Mohamed, A.F., Osman, O.O., Ghazaly, N.M., 2019. “Study of friction coefficient of wind turbine brake system under environmental conditions”. International Journal of Advanced Science and Technology 28(12), 167-177.

Moubray, J. (2001). Reliability-Centered Maintenance.

Schijve, J. (2009). Fatigue of Structures and Materials.

Taiwan Power Company, "Offshore Wind Farm Operation Reports", 2023, Internal Technical Report.

Talati, F., Jalalifar, S., 2009. “Analysis of heat conduction in a disk brake system”. Heat and Mass Transfer 45(8), 1047-1059.

Travaglia, C.A.P., Lopez, L.C.R., 2014. “Friction material temperature distribution and thermal and mechanical contact stress analysis”. Engineering 6(13), 1017-1036.